JVI Journals.ASM.org

Human Rotavirus-Specific IgM Memory B Cells Have Differential Cloning Efficiencies and Switch Capacities and Play a Role in Antiviral Immunity *In Vivo*

Carlos F. Narváez,[a,b,c] Ningguo Feng,[b] Camilo Vásquez,[a] Adrish Sen,[b] Juana Angel,[a] Harry B. Greenberg,[b] and Manuel A. Franco[a]

Instituto de Genética Humana, Facultad de Medicina, Pontificia Universidad Javeriana, Bogotá, Colombia[a]; Departments of Medicine and Microbiology & Immunology, Stanford University School of Medicine, Stanford, California, USA[b]; and Facultad de Salud, Programa de Medicina, Universidad Surcolombiana, Neiva, Colombia[c]

Protective immunity to rotavirus (RV) is primarily mediated by antibodies produced by RV-specific memory B cells (RV-mBc). Of note, most of these cells express IgM, but the function of this subset is poorly understood. Here, using limiting dilution assays of highly sort-purified human IgM$^+$ mBc, we found that 62% and 21% of total (non-antigen-specific) IgM$^+$ and RV-IgM$^+$ mBc, respectively, switched *in vitro* to IgG production after polyclonal stimulation. Moreover, in these assays, the median cloning efficiencies of total IgM$^+$ (17%) and RV-IgM$^+$ (7%) mBc were lower than those of the corresponding switched (IgG$^+$ IgA$^+$) total (34%) and RV-mBc (17%), leading to an underestimate of their actual frequency. In order to evaluate the *in vivo* role of IgM$^+$ RV-mBc in antiviral immunity, NOD/Shi-scid interleukin-2 receptor-deficient (IL-2Rγ^{null}) immunodeficient mice were adoptively transferred highly purified human IgM$^+$ mBc and infected with virulent murine rotavirus. These mice developed high titers of serum human RV-IgM and IgG and had significantly lower levels than control mice of both antigenemia and viremia. Finally, we determined that human RV-IgM$^+$ mBc are phenotypically diverse and significantly enriched in the IgM^{hi} IgD^{low} subset. Thus, RV-IgM$^+$ mBc are heterogeneous, occur more frequently than estimated by traditional limiting dilution analysis, have the capacity to switch Ig class *in vitro* as well as *in vivo*, and can mediate systemic antiviral immunity.

Rotavirus (RV) is the most common cause of severe gastroenteritis in children less than 5 years old worldwide (50). Although two safe and effective, live, attenuated oral RV vaccines were licensed for use in humans in 2006, the long-term impact of these vaccines on the reduction of RV-induced severe gastroenteritis, especially in the poorest countries, has not been completely established (12, 72). Recent studies have shown lower levels of protection in vaccinated children from developing countries in Asia and Africa, with a higher incidence of RV gastroenteritis in these children compared to vaccinated children in the United States (42, 43, 60, 74). A better understanding of the mechanisms of immune protection after natural infection or vaccination is key to development of more effective third-generation vaccination strategies against RV (3).

B cells are a critical component of protective immunity against RV: B cell-immunodeficient mice are unable to generate long-term protection against this virus (23); B and/or T cell-immunodeficient children can be chronically infected with RV, and these chronic infections may occur extraintestinally (24). Moreover, several studies have correlated increased serum and mucosal antibody levels with protection in children (13, 66). In humans, naive B cells and three main subsets of memory B cells (mBc) can be readily identified in the circulation, based on the surface expression of CD19, IgD, IgM, and CD27: naive B cells (CD19$^+$ IgD$^+$ IgM$^+$ CD27$^-$), switched mBc (CD19$^+$ IgD$^-$ IgM$^-$ CD27$^+$), IgM$^+$ mBc (CD19$^+$ IgD$^+$ IgM$^+$ CD27$^+$), and CD27$^-$ mBc (CD19$^+$ IgD$^-$ IgM$^-$ CD27$^-$) (18, 33, 70). Two methods have been commonly used to quantify and characterize mBc. In the commonly used limiting dilution assay (LDA), the antibodies produced by individual mBc are evaluated after polyclonal stimulation (37). Quantification and determination of the phenotypes of total (non-antigen-specific) and antigen-specific mBc can also be performed with flow cytometry-based assays (FCA) (39, 45). To characterize the phenotype of mBc that express RV surface Ig, we and others have used an FCA (29, 51, 64, 73). The principle of this assay consists of the specific binding of fluorescent RV recombinant virus-like particles (VLPs) that express on their surface the immunodominant RV structural protein VP6 and inside contain green fluorescent protein (GFP) linked to the amino terminus of VP2 (11). After using this FCA, we recently reported that the majority of RV-mBc express IgM (53). In contrast, in an LDA, RV-mBc were lower in frequency and predominantly expressed IgG rather than IgM. This lack of correlation was only seen for RV-mBc: tetanus toxoid-specific mBc predominantly expressed IgM in both assays (53). Although a role for IgM$^+$ mBc in the immune responses against bacteria like *Streptococcus pneumoniae* has been described (35, 58), the role of this subset in antiviral and antirotaviral immunity in particular is unknown.

In order to better understand the role RV IgM$^+$ mBc, we have more carefully quantified and further characterized human RV IgM$^+$ mBc and determined that they have a differential *in vitro* switching capacities and cloning efficiencies and are enriched in the CD27$^+$ IgM^{hi} IgD^{low} subset. Moreover, by using an immunodeficient mouse model, we determined that transferred human IgM$^+$ mBc can also switch to secrete IgG *in vivo* and that these cells confer functional RV immunity to recipient mice.

Received 12 June 2012 **Accepted** 23 July 2012
Published ahead of print 1 August 2012
Address correspondence to Manuel A. Franco, mafranco@javeriana.edu.co.
H.B.G. and M.A.F. contributed equally to the work as senior authors.

doi:10.1128/JVI.01466-12

MATERIALS AND METHODS

Isolation of B cells by rosette formation and purification of B cell subsets by fluorescence-activated cell sorting (FACS). This study was carried out in accordance with Stanford University Medical School Policies on Human Subjects Research. Buffy coats from deidentified healthy donors were provided by the Stanford University Blood Bank and used within 3 h or less of isolation. Prior studies indicated that virtually all humans are exposed to RV in the first 3 years of life, as indicated by the presence of rotavirus-specific antibodies in the circulation (65). Total circulating B cells were obtained by negative selection by rosette formation (StemCell Biotech, Vancouver, Canada). The median (range) purity of $CD19^+$ cells after selection was 90% (87 to 96%). In some experiments, positive selection with anti-CD19-labeled magnetic microbeads (Miltenyi Biotec, Auburn, CA) was used with comparable results.

Total B cells were washed twice with RPMI supplemented with 10% fetal bovine serum, 2 mM L-glutamine, 100 U/ml penicillin, 100 μg/ml streptomycin, 0.1 mM nonessential amino acids, 1 mM sodium pyruvate, and 0.05 mM β-mercaptoethanol (complete medium). All reagents were from Gibco-BRL (Gaithersburg, MD). Subsequently, 1×10^7 to 4×10^7 purified B cells were stained with anti-CD3/CD14/CD16–peridinin chlorophyll protein (PerCP)-Cy5.5 (to be used as a dump channel; Becton, Dickinson [BD], San Jose, CA), anti-CD19–phycoerythrin (PE)-Cy7 (SJ25C1 clone; BD), anti-CD27–PE (MT271 clone; BD), goat anti-IgA conjugated to allophycocyanin (APC; Jackson ImmunoResearch, West Grove, PA), and goat anti-IgG APC (Jackson ImmunoResearch) and sorted by FACS using a BD FACS ARIA II apparatus. At least 1×10^6 naive B cells, IgM^+ mBc, and switched mBc were isolated (5). The median (range) purities of the naive B cells, IgM^+ mBc, and switched mBc were 96% (94 to 98%), 94% (91 to 98%), and 92% (90 to 97%), respectively. The sorting strategy is shown in Fig. 1A. After sorting, the B cell subsets were counted by trypan blue exclusion staining and immediately used for the LDA. Cell viability was typically higher than 90% for the three subsets.

Antigen-specific FCA. The frequencies of RV-mBc were determined as previously reported (53). RV VP2 and VP6 VLPs containing GFP (GFP-VLPs) were generated as previously described (11). RV VP6 is an immunodominant protein, and the majority of human RV-specific B cells bind to VP6. Negatively purified total B cells were washed once with phosphate-buffered saline (PBS), 2% fetal bovine serum, 0.02% sodium azide (staining buffer), and then incubated with GFP-VLPs (0.8 μg/test; concentration determined by titration on anti-VP6 mouse hybridoma cells) for 45 min at 4°C in the dark. The cells were then washed with staining buffer and stained with the same antibody panel used for sorting circulating mBc subsets: anti-CD19–PE-Cy7, anti-CD27–PE, and anti-IgG–APC and anti-IgA–APC. Of note, in six experiments, anti-IgM, -IgG, and -IgA antibodies conjugated to APC were used independently. After 30 min of incubation, cells were washed with staining buffer and fixed with 1% paraformaldehyde (Electron Microscopy Sciences, Washington, PA). At least 300,000 purified B cells were acquired on the FACS Aria II or LSR II cytometers with DIVA software (BD, San Jose CA). In a subset of volunteers, B cells purified as described above for the sorting experiments were also stained with anti-human CD3–Pacific Blue, anti-CD14–V500, anti-CD20–PerCP-Cy5.5, anti-CD27–PE Cy7, anti-IgD–APC-H7, anti-CD21–PE, anti-IgM–Alexa Fluor 700, and anti-CD43–APC (all from BD, San Jose, CA) for 30 min at 4°C. Cells were then washed with staining buffer and fixed with 1% paraformaldehyde.

Limiting dilution assay. FACS-sorted naive, IgM^+ mBc, and switched mBc were distributed in serial dilutions from 20,000 to 0.3 cells/well in a volume of 200 μl, using 24 replicate cultures per dilution. Cells were stimulated with 2.5 μg/ml of CpG (ODN 2006; InvivoGen, San Diego, CA), 10 ng/ml human recombinant IL-2 and 10 ng/ml human recombinant IL-6 (both from R&D Systems, Minneapolis, MN), 15 ng/ml IL-10 (Pharmingen) plus NIH 3T3 murine fibroblasts (a gift from E. C. Butcher, Stanford University, Stanford, CA). The NIH 3T3 feeder cells were previously treated with 50 μg/ml of mitomycin C (Sigma-Aldrich) for 30 min, washed exhaustively, and then used at a concentration of 5,000 cells/well. After 5 to 7 days of culture, the supernatants were collected and stored at −20°C. In some experiments, cells were also collected to identify antibody-secreting cells (ASCs) by enzyme-linked immunosorbent spot (ELISPOT) assay or flow cytometry (FC) as described below.

ELISA for detection of total and RV-specific IgA, IgG, and IgM in culture supernatants. The supernatants from the 24 culture replicates from each of three sorted B cell subsets were thawed and tested for the presence of total and RV-specific IgM, IgG, and IgA and, in some experiments, tetanus toxoid-specific IgM and IgG in an enzyme-linked immunosorbent assay (ELISA), as previously described with minor modifications (53). Immulon 2 ELISA plates (Dynex Technologies, Chantilly, VA) were coated with either a 1/2,000 dilution of anti-whole human Ig (Sigma-Aldrich), 0.4 μg/ml of GFP-VLP, 2.5 μg/ml of tetanus toxoid (Staten Serum Institute, Denmark), or PBS as negative control and incubated overnight at 4°C. After discarding the coating solutions, 150 μl/well of 5% BLOTTO was added, and the plates were incubated at 37°C for 1 h. The BLOTTO solution was then discarded, and 70 μl/well of B cell culture supernatant was deposited in each well. After a 2-h incubation at 37°C, the plates were washed three times with 0.1% Tween 20 in PBS (washing buffer), and 70 μl of biotin-labeled goat anti-human IgA, IgG, or IgM (Kirkegaard & Perry Laboratories [KPL], Gaithersburg, MD) diluted in 2.5% BLOTTO was added and incubated for an additional 1 h at 37°C. After three washes with washing buffer, 70 μl/well of a 1/1,000 dilution of streptavidin-peroxidase (Kirkegaard & Perry Laboratories) in 2.5% BLOTTO was added, and the plates were again incubated for 1 h at 37°C. After three washes with PBS-Tween 20, plates were developed using 70 μl/well of tetramethyl benzidine substrate (TMB; Kirkegaard & Perry). The reaction was stopped by the addition of 17.5 μl/well of 2 M sulfuric acid. Absorbance was read at a wavelength of 450 nm on an ELISA plate reader. Of note, the presence of total or antigen (Ag)-specific IgM, IgG, and IgA in the same supernatant can be detected in the LDA. In some experiments, unstimulated sorted, naive, IgM^+ mBc and switched mBc were used as negative controls, and secreted antibodies were not detected in these supernatants (data not shown).

Phenotype and intracellular Ig expression of purified B cell subsets. After culture for LDA, a fraction of the cells was used to quantify ASCs. Cells were washed twice with staining buffer and stained with anti-CD19–APC-Cy7 (SJ25C1 clone; BD), anti-CD20–PE-Cy7 (L27 clone; BD), anti-CD27–PE (M-T271 clone; BD), anti-CD38–PerCP-Cy5.5 (HIT2 clone; BD), anti-IgD–fluorescein isothiocyanate (FITC; IA6-2 clone; BD), and goat anti-human IgM–APC (Jackson ImmunoResearch) and incubated at 4°C for 30 min. Cells were then washed, fixed, and analyzed by FC. Another fraction of cells was used to detect surface and intracellular Ig. These cells were washed with staining buffer and incubated with anti-CD19–APC-Cy7, anti-CD20–PE-Cy7, and anti-CD27–PE for 30 min. Cells were washed with staining buffer, then treated with 250 μl cytofix/cytoperm (BD Pharmingen), and incubated for 20 min at 4°C. Cells were then washed twice with perm/wash buffer (BD Pharmingen), and anti-IgG–FITC and anti-IgA–APC (Jackson ImmunoResearch) were added for 30 min at 4°C. Cells were then washed, resuspended in perm/wash buffer, and analyzed by FC.

Two-color ELISPOT. After 5 to 7 days of culture, LDA plates were centrifuged, and the highly purified naive, IgM^+ mBc, and switched mBc were collected and washed twice with complete medium. Total ASCs present in the cultures were measured in a two-color ELISPOT assay as previously described (48, 54). Briefly, 96-well plates (Immobilon P membrane; MAIPN4510; Millipore, Billerica, MA) were coated with affinity-purified goat anti-human IgA, IgG, plus IgM (heavy and light chains; KPL, Gaithersburg, MD) at a concentration of 4 μg/ml in sterile PBS. Wells were coated with PBS as a negative control. Plates were incubated overnight at 4°C and blocked for 2 h at 37°C with complete medium prior to use. Stimulated cells were suspended in complete medium containing 6.3 μg/ml peroxidase-conjugated goat anti-human IgM antibody (Sigma, St. Louis, MO) and 0.5 μg/ml of phosphatase-conjugated goat anti-human IgG antibody (KPL), distributed into ELISPOT plates, prepared as de-

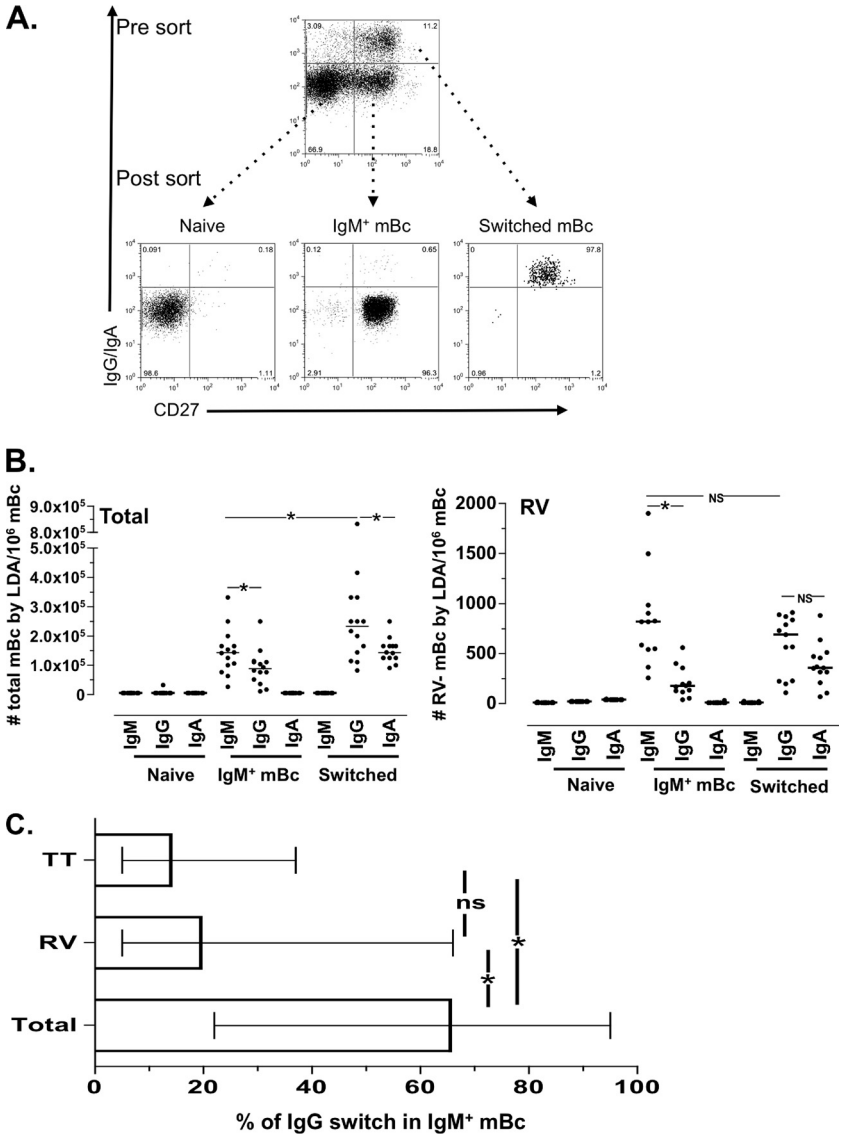

FIG 1 Sort-purified total and RV IgM$^+$ mBc switch isotype to IgG *in vitro*. (A) Starting from rosette-enriched B cells, naive, IgM$^+$, and switched mBc were sort purified based on their expression of CD19, CD27, IgG, and IgA. Results of 1 representative experiment of 14 performed experiments is shown. Serial dilutions (24 replicate wells per dilution) of purified naive, IgM$^+$ mBc, and switched mBc were stimulated as described in Materials and Methods and cultured for 7 days. Total and RV-specific IgM, IgG, and IgA were measured in the supernatants by ELISA. (B, left panel) Number of total IgM-, IgG-, and IgA-secreting B cells in the indicated cultures. (Right panel) Number of RV-specific IgM-, IgG-, and IgA-secreting B cells in the indicated cultures. The lines represent the medians. An asterisk indicates a statistically significant difference ($P \leq 0.03$, Wilcoxon test). (C) Frequencies of total, RV, and tetanus toxoid (TT) IgM$^+$ mBc that switched isotype to IgG *in vitro*. The medians and ranges are shown. An asterisk indicates a statistical differences ($P \leq 0.02$, Mann-Whitney test). ns, nonsignificant difference.

scribed above, and incubated 4 h at 37°C in 5% CO_2. Plates were washed with PBS, developed with an AEC substrate kit for peroxidase (Vector, Burlingame, CA), and subsequently developed with a blue alkaline phosphatase substrate kit (Vector). Human IgM ASCs were visualized as red spots, and IgG ASCs appeared as blue spots in the same wells. IgA ASCs were detected in independent wells. The total ASCs per well was determined by counting the spots under a dissecting microscope. Background ASCs detected in the wells coated with PBS were subtracted from the quantities of ASCs in treated wells.

Adoptive transfer of the sorted human IgM$^+$ mBc subset. This study was carried out in accordance with the recommendations provided in the *Guide for the Care and Use of Laboratory Animals* of the National Research Council of the National Academy of Science (49). All mouse experiments were approved by the Animal Care Committee of Stanford University Medical School.

Sixteen female 6- to 8-week-old NOD/Shi-scid IL-2Rγ^{null} immunodeficient mice were purchased from Taconic Corporation (Oxnard, CA) and maintained in the VA Palo Alto Healthcare System vivarium.

Adoptive transfer of human lymphocytes was performed as previously reported (46). Four buffy coats were provided by the Blood Bank of Stanford University. From each buffy coat, whole peripheral blood mononuclear cells (PBMCs) and B cells were purified by use of a Ficoll gradient and negative selection by rosette formation, respectively. PBMCs were stained with anti-CD19–PE, anti-CD3–FITC, and CD4–PerCp-Cy5.5 to determine the frequencies of these cell populations. The medians (ranges) of B and CD4$^+$ T cells in the PBMCs studied were 10.4% (6.5 to 15.5%)

and 34% (17 to 45%), respectively. Purified B cells were stained with anti-CD19–PE-Cy7, anti-CD27–PE, and anti-IgA/IgG–APC and sorted on the FACS Aria II apparatus as described above. Before sorting, the IgM^+ mBc subset ($CD27^+$ IgA^- IgG^-) corresponded to 19.8% (5 to 23%) of total B cells. After sorting, the purity of the IgM^+ mBc was 98% (95 to 99%), and less than 0.5% of these cells were IgA^+ IgG^+. To produce B cell-depleted PBMCs (Bc-dPBMCs), microbeads coupled with an anti-CD19 antibody (Miltenyi Biotec) were used. After depletion, less than 0.4% of the Bc-dPBMCs expressed CD19.

Two million purified IgM^+ mBc were combined with homologous Bc-dPBMCs in a ratio that restored the proportion of $CD4^+$ T cells to that in the original PBMC population. These cells were diluted in sterile PBS and injected intraperitoneally (i.p.) into NOD/Shi-scid IL-2Rγ^{null} mice. Control mice (4 animals per group) received an equivalent number of unfractionated PBMCs, Bc-dPBMCs alone, or sterile PBS. Immediately after lymphocyte transfer, all mice were infected with wild-type homologous virulent murine RV (EC_{WT}) with a 50% infectious dose of 100, as previously described (22). Stool samples were collected daily from all mice and stored at −20°C. Fifteen days after transfer, mice were bled and serum was stored at −20°C. Levels of total human Igs and RV-specific and tetanus toxoid-specific Igs were determined by ELISA as described above or as previously described (53).

Detection of RV-Ag in serum and stool. The relative quantities of VP6 were detected by ELISA in mouse serum and stool specimens as previously reported, with some modifications (32, 47). Briefly, Immulon 2 ELISA plates (Dynex Technologies, Chantilly, VA) were coated with murine monoclonal antibody to VP6 (1E11 clone) at a 1/2,000 dilution in sterile PBS. Sterile PBS alone was used as a negative control. Plates were incubated overnight at 4°C. The next day, after 1 h of blocking with 5% BLOTTO, serum or stool samples were diluted and incubated for 2 h at 37°C. Wells were then washed, and guinea pig anti-RV serum (1/4,000 dilution) was added, incubated for an additional 1 h at 37°C, washed, and then developed with a biotinylated goat anti-guinea pig serum (Vector, Burlingame, CA) followed by a 1/1,000 dilution of streptavidin-peroxidase (KPL) and TMB substrate (KPL). The reaction was stopped by the addition of 17.5 μl of 2 M sulfuric acid. Absorbance was read at a wavelength of 450 nm on an ELISA plate reader.

Detection of RV NSP5-RNA in serum by using quantitative reverse transcription-PCR (RT-PCR). Detection of RV-RNA in the serum was performed as described previously, with minor variations (56). RNA was purified from murine serum samples with the Qiagen viral RNA purification kit per the manufacturer's recommendations. Purified RNA was denatured in the presence of 10% (vol/vol) dimethyl sulfoxide at 95°C for 5 min and snap-chilled on ice. The denatured RNA was then used as a template for reverse transcription using random hexamers and the SuperScript III first-strand synthesis kit (Invitrogen, Carlsbad, CA) per the manufacturer's protocol. The cDNA was used for a preamplification PCR for 10 cycles on an Mx3005P real-time cycler (Agilent, Santa Clara, CA) using a previously described TaqMan assay for the gene encoding NSP5 (56) at a 0.2× final concentration and the FAST II PCR mix (Agilent) under the following cycling conditions: 95°C for 2 min, followed by 10 cycles of 95°C for 10 s and 60°C for 30 s. The preamplification reaction mixtures were then diluted 5-fold in sterile water, and 2 μl was used for a second PCR using 1× TaqMan assay mixture for 30 cycles and the PCR conditions described above. As positive controls, we used RV RNA purified from 0.025×10^4 to 2.5×10^4 PFU of a purified rhesus rotavirus three-layered particle (TLP) stock obtained by ultracentrifugation on cesium gradients as previously described (20).

Statistical analysis. To determine frequencies in the LDA, a least-squares linear regression was used to fit a line with the frequencies of negative cultures. The R^2 value (≥0.83) and P value (≤0.05) were calculated for the best-fit line. The frequencies of total and Ag-specific mBc were calculated from a 37% interpolation of the titration curve which, according to the Poisson distribution, represented the number of wells containing a single precursor, as previously described (2, 37). The possibility that more than one Ig isotype might have been produced by a single B cell in the sorted switched mBc cultures was evaluated by comparing the expected and observed frequencies of IgG-positive and IgA-positive wells using Fischer's exact test (38).

FC analysis was performed using FlowJo software (Treestar, Ashland, OR). Statistical analyses were performed with SPSS 18.01 (Chicago, IL) and Prism 5.0 using nonparametric tests. Differences between two independent groups were evaluated with Mann-Whitney tests. Differences between paired results were compared with the Wilcoxon test. Significance was established if the P value was less than 0.05. Data are shown as medians and ranges unless otherwise noted.

RESULTS

Total and RV-mBc switch *in vitro* at different rates. To further characterize IgM^+ mBc, we first determined if total and RV IgM^+ mBc have the capacity to switch isotype *in vitro*. To this end, sort-purified $CD27^+$ IgA^- IgG^- (IgM^+ mBc) (Fig. 1A) were evaluated by LDA (Fig. 1B). For comparison, switched mBc ($CD27^+$ IgG^+ IgA^+) and naive B cells ($CD27^-$ IgG^- IgA^-) were also studied. We evaluated the purity of the sorted populations based on expression of sorting markers (Fig. 1A, postsort [$n = 14$]) and the expression of IgD and IgM ($n = 7$) (data not shown). After sorting, as expected, naive B cells, IgM^+ mBc, and switched mBc contained a median (range) of double-positive IgM^+ IgD^+ B cells of 93% (90 to 97%), 90% (87 to 97%), and 1% (0 to 3%), respectively (data not shown).

For the LDA, purified subsets of B cells were stimulated with a cocktail of CpG 2006, IL-2, IL-6, IL-10, and mitomycin C-treated NIH 3T3 feeder cells, a strategy previously shown to be optimal for detection of RV-mBc and tetanus toxoid-mBc (2, 53). Frequencies of total (non-antigen-specific) cells and RV-mBc were evaluated by LDA (Fig. 1B) in the three purified B cell subsets of Fig. 1A. As expected, no total or RV-mBc were detected in the LDA cultures of naive B cells (Fig. 1B). Given the high purity of the IgM^+ mBc used for the LDA cultures (Fig. 1A and data not shown), we concluded that a median of 62% of total and 21% of RV-IgM^+ mBc switched in culture to secrete IgG during the 5- to 7-day culture period (Fig. 1C). Of note, in none of these cultures were significant numbers of total or RV-specific IgA-secreting cells detected (Fig. 1B). For comparison, we also measured the number of tetanus toxoid IgM- and IgG-secreting cells in the LDA of highly purified human IgM^+ mBc cultures. A median (range) of 16% (6 to 37%) tetanus toxoid IgM^+ mBc switched to IgG, and this frequency was lower and significantly different from the proportion of total mBc that switched ($P = 0.02$, Mann-Whitney test), but these findings were not different from the proportion of RV IgM^+ mBc that switched (Fig. 1C).

In the cultures of purified switched mBc, a significantly higher frequency of mBc secreted total IgG than IgM or IgA ($P = 0.03$ and 0.02, respectively [Wilcoxon test]) (Fig. 1B). Significant differences in frequencies of cells secreting IgG, or IgA were not seen when RV-specific mBc were analyzed (Fig. 1B). As expected, total IgM or RV IgM-producing cells were not detected in these cultures (Fig. 1B). To analyze the potential IgG-to-IgA switch in the cultures of purified switched B cells, the frequency of wells in which both IgG and IgA was detected were compared to the frequency expected by chance in plates in which cells were close to one precursor per well (37). As shown in Table 1, the IgG-to-IgA switch occurred in 29% and 15% of total and RV-specific switched mBc, respectively.

To confirm and extend these results, naive, IgM^+, and switched

TABLE 1 IgG-to-IgA switch in sorted CD27$^+$ IgG$^+$ or CD27$^+$ IgA$^+$ total switched and RV-switched mBc populations

Switched mBc population and expt no.	No. of B cells/well	No. of wells[a] containing indicated Ig(s)				Expected no. of wells with P > 1[b]	Fisher test *P* value[c]	% switched
		IgG	IgA	IgG + IgA	Neither IgG nor IgA			
Total switched mBc								
1	3	21	13	12	2	9	0.61	17
2	7	18	12	12	6	5	0.16	40
3	4	14	13	12	9	3	0.03[&]	64
4	6	12	7	3	8	4	0.5	0
5	5	16	15	13	6	5	0.04[&]	51
6	3	11	7	4	10	3	0.5	13
7	3	15	9	6	6	5	0.5	8
8	2	11	9	5	9	3	0.39	17
9	5	16	8	8	8	4	0.23	27
10	2	19	13	13	5	6	0.1	39
11	5	15	9	9	9	3	0.1	39
12	5	15	14	10	5	6	0.28	29
13	5	11	14	7	7	4	0.31	26
14	7	10	7	5	12	2	0.25	32
Global[d]								29
RV-switched mBc								
1	1,650	16	6	5	7	4	1	5
2	1,875	15	4	2	7	4	0.6	0
3	958	8	10	4	9	3	1	11
4	5,833	13	7	5	9	3	0.7	15
5	2,333	18	6	4	4	6	0.7	0
6	1,250	6	10	3	11	2	1	13
7	2,500	15	8	5	6	5	1	1
8	1,250	14	12	11	9	3	0.07	57
9	1,250	8	9	6	13	2	0.2	56
10	312	7	7	4	14	1	0.3	40
11	2,500	6	11	3	10	3	1	6
12	625	8	7	3	12	2	0.5	14
13	2,175	14	11	9	7	4	0.3	34
Global[d]								15

[a] From a total of 24 wells.
[b] The frequency of wells for each experiment expected to contain more than one precursor (P > 1) was calculated as follows: 1 − [the frequency of wells with 1 P (calculated according to the Poisson distribution)] − [the observed frequency of wells with 0 P]. This value was then divided by 2 to estimate the expected number of wells in which cells secreting both IgA and IgG were present, taking into account that wells with P = 2 could be of the same or different isotypes.
[c] &, statistically significant difference between the expected number of wells with more than one precursor and the frequency of wells in which cells secreting both IgG and IgA were detected.
[d] The global percentage switch was calculated by taking into account all experiments for a test group (i.e., total or RV-switched mBc).

mBc were collected after LDA culture and stained to measure the expression of surface and intracellular IgD, IgM, IgG, and IgA. As expected, after 5 to 7 days of culture, the majority of naive B cells expressed IgM and IgD (data not shown). In contrast, in the IgM$^+$ subset, the expression of IgD was substantially downregulated, with a median (range) of only 26% (21 to 49%) of cells coexpressing IgM and IgD after 7 days of culture. In addition, a significant fraction of IgM$^+$ mBc, median (range) 15% (6 to 35%), lost expression of IgD and IgM altogether (data not shown). As expected, switched mBc did not express IgD or IgM. Consistent with the above and LDA results, a median (range) of 20% (8 to 40%) and 71% (53 to 90%) of cells from the IgM$^+$ mBc and from switched mBc, expressed IgG after 7 days of culture, respectively (data not shown). Also in agreement with the LDA results (Fig. 1B), very few, if any, IgA$^+$ B cells were detected in the IgM$^+$ mBc LDA cultures by FC.

Cloning efficiency of purified IgM$^+$ and switched memory B cells. To determine the cloning efficiencies of total IgM$^+$ mBc and switched mBc, the number of sorted mBc detected by LDA was divided by the number of cultured cells and multiplied by 100. To determine the cloning efficiency of virus-specific mBc (Fig. 2A), the number of RV-mBc detected by LDA was expressed as a percentage of those detected by FCA (Fig. 2B). The cloning efficiency of switched total and switched RV-mBc was significantly higher than the number of total and RV IgM$^+$ mBc ($P = 0.02$ and 0.04 [$n = 14$ and 11], respectively; Wilcoxon tests) (Fig. 2A), even when the switching from IgG to IgA in switched mBc cultures (Table 1) was taken into account to calculate cloning efficiencies. Moreover, compared to the cloning efficiencies of total IgM and total switched mBc, the cloning efficiencies of the corresponding RV-mBc were lower, although this difference was only significant for the IgM$^+$ mBc (Fig. 2A). These findings were supported by a subset of experiments ($n = 6$) in which the cloning efficiency of mBc was calculated by staining separately for IgM, IgG, and IgA (data not shown). Moreover, similar results were obtained in two experiments in which switched mBc were sorted as IgD$^-$ IgM$^-$ B cells (data not shown). This last result suggests that our results

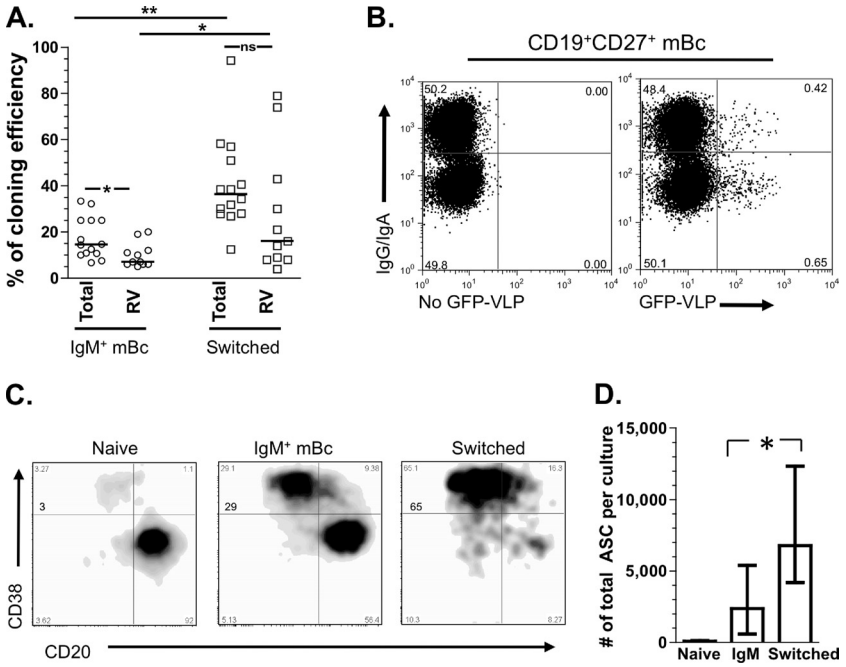

FIG 2 IgM$^+$ mBc have lower cloning efficiencies than switched mBc. (A) Cloning efficiencies of total and RV IgM$^+$ mBc and switched mBc. Total mBc cloning efficiencies were calculated based on the percentage of the numbers of mBc obtained in the LDA. The cloning efficiency of RV-mBc was calculated as the fraction of the cells used for the sorting experiments stained with GFP-VLP (shown in panel B). Lines represent the medians. One and two asterisks represent statistically significant differences in the frequency of mBc between IgM$^+$ mBc and switched mBc ($P = 0.04$ and 0.02, respectively; Wilcoxon test). (C) The expression of plasmablast markers in naive, IgM$^+$ mBc, and switched mBc after 7 days of culture was evaluated by FC. One representative experiment of seven performed is shown. (D) Frequencies of total IgM, IgG, and IgA ASCs generated after culture of each indicated subset, as detected by two-color ELISPOT. Medians and ranges of nine experiments are shown. The asterisk indicates a statistically significant difference ($P = 0.01$, Mann-Whitney test).

were probably not influenced by our sorting strategy, in which cells were sorted with antibodies directed at the B cell receptor (BCR). In conclusion, circulating human total and RV IgM$^+$ mBc have lower cloning efficiencies by LDA than their corresponding switched mBc, and a lower cloning efficiency with respect to total IgM$^+$ mBc was detected with RV IgM$^+$ mBc, supporting the notion that RV-mBc are a unique subset of IgM$^+$ mBc.

Next, to confirm and extend these differences in cloning efficiency rates, the phenotypes and numbers of ASCs obtained at the end of the LDA were evaluated by FC and ELISPOT, respectively. Significantly higher frequencies of B cells with the phenotype of ASCs were found in the cultures of switched cells compared to those from the IgM$^+$ mBc subset (Fig. 2C). The medians (ranges) of cells with an ASCs phenotype (CD19$^+$ CD20^{low} CD38^{high}) in cultures of IgM$^+$ and switched mBc were 30% (12 to 45%) and 58% (16 to 72%), respectively ($P = 0.03$, Wilcoxon test; $n = 7$). Consistent with these results, the numbers of total IgM$^+$, IgG$^+$, and IgA$^+$ ASCs produced in the LDA cultures of switched mBc and detected by ELISPOT were 3-fold greater than that of IgM$^+$ mBc (Fig. 2D). Very few ASCs were identified by FC or ELISPOT in cultures of naive B cells (Fig. 2C and D, respectively).

Human memory B cells that express IgM can switch to IgG *in vivo* and reduce levels of RV antigenemia and viremia in immunodeficient mice infected with RV. Given the high frequency of RV-IgM$^+$ mBc *in vivo* and their substantial ability to switch *in vitro*, we next sought to determine if circulating human IgM$^+$ mBc could switch in the context of a viral infection *in vivo* and if such a switch was associated with any functional activity. Highly purified (median purity, 98%) human IgM$^+$ mBc were mixed with autologous Bc-dPBMCs (used to provide antigen-presenting cells) and transferred i.p. into NOD/Shi-scid IL-2Rγ^{null} adult mice. Three additional groups of mice were treated with unfractionated PBMCs, Bc-dPBMCs alone, or PBS and served as controls. Immediately after transfer, all four groups of mice were infected orally with virulent murine rotavirus (EC_{WT}). On day 15 postinfection, significant quantities of human total IgM, IgG, and IgA were found in the sera of mice treated with unfractionated PBMCs (Fig. 3A). Consistent with *in vitro* results (Fig. 1B and data not shown), both total human IgM and human IgG, but not human IgA, were detected in the serum of mice transferred highly purified IgM$^+$ mBc (Fig. 3A). Interestingly, high titers of serum RV IgM and RV IgG, but not RV IgA, were also detected in mice given IgM$^+$ mBc (Fig. 3A). As a control, human tetanus toxoid-specific IgM, IgG, and IgA were also quantified. Mice given whole PBMCs developed low titers of serum tetanus toxoid-specific IgG, but no tetanus toxoid IgM was detected (Fig. 3A). In mice transferred Bc-dPBMCs or PBS, human Igs were not detected (Fig. 3A).

Self-limited RV antigenemia and viremia are frequently found in acutely infected mice and children (7, 19). Therefore, we examined the role of human IgM$^+$ mBc in the control of RV antigenemia. Fifteen days after oral RV infection, high serum levels of RV-VP6 antigen were detected in mice given PBS IP (Fig. 3B). Mice dosed IP with human whole PBMCs or purified IgM$^+$ mBc had significantly reduced levels of serum RV-VP6. Mice given Bc-dPBMCs had intermediate levels of circulating RV-VP6 (Fig. 3B). As shown in Table 2, the levels of circulating RV-RNA in the serum determined by quantitative RT-PCR in a fraction of mice correlated with the ELISA results and confirmed that human

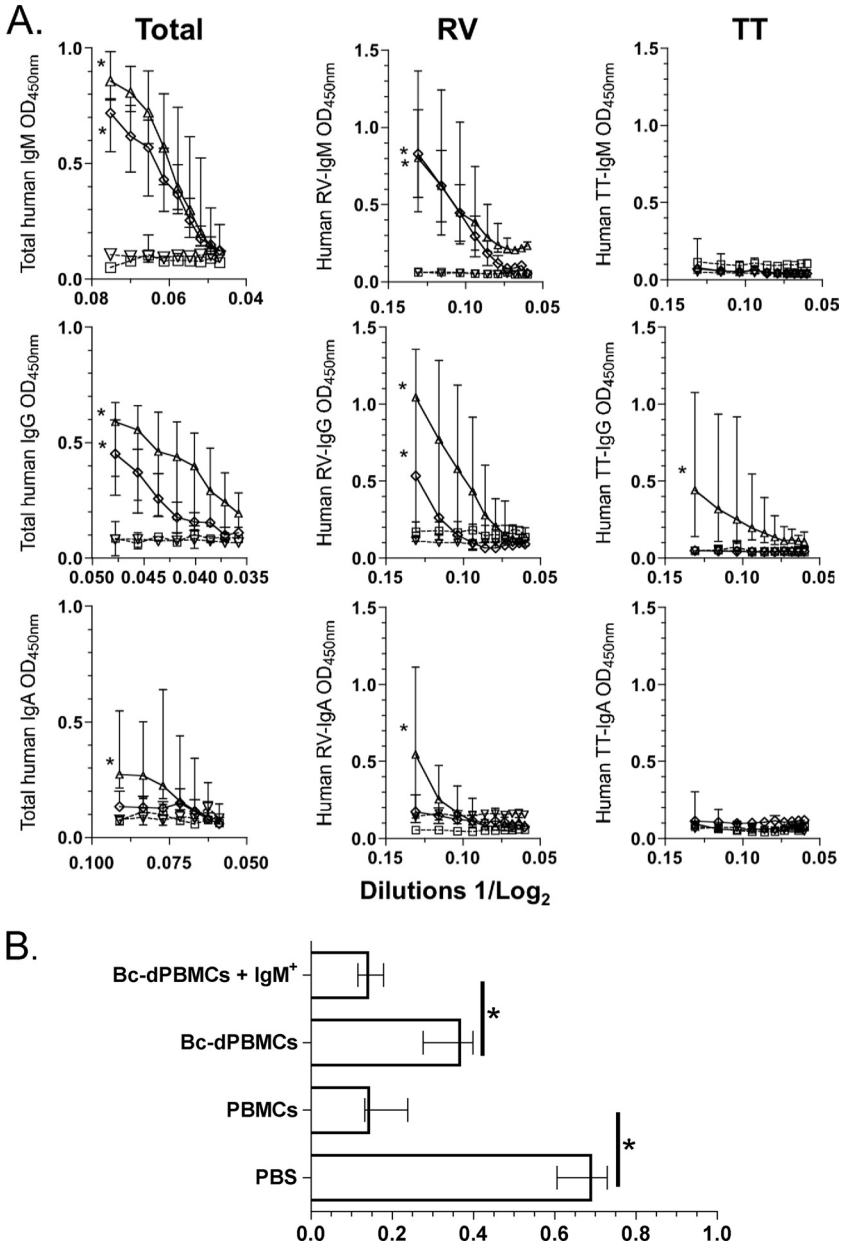

FIG 3 Total and RV IgM$^+$ mBc switch to IgG isotype frequencies *in vivo*. (A) Immunodeficient NOD/Shi-scid IL-2Rγ^{null} adult mice were i.p. inoculated with PBS (□, dashed line), PBMCs (△, continuous line), Bc-dPBMCs (▽, dashed line), or Bc-dPBMCs plus highly purified IgM$^+$ mBc (◇, continuous line) and immediately infected orally with the murine EC_{WT} strain RV. Fifteen days after infection, relative quantities of human total, RV-specific, and tetanus toxoid (TT)-specific (as a control Ag) IgM, IgG, and IgA were determined in the serum by ELISA. Optical densities (at 450 nm) of serial dilutions of serum are presented on a $\log_2$ scale. Each point represents the median ($n = 4$), and the lines represent the range for each dilution. An asterisk represents a statistically significant difference ($P < 0.05$, Mann-Whitney test). (B) Human IgM$^+$ mBc are involved in clearing RV antigenemia. Relative quantities are shown for RV VP6 detected by ELISA (optical density at 450 nm [OD_{450}]) in the serum of mice that were transferred human cells (or PBS as a control). The bars represent the medians, and lines represent the ranges ($n = 4$). An asterisk indicates a significant difference ($P = 0.02$, Mann-Whitney test).

IgM$^+$ mBc can reduce levels of antigenemia and viremia in chronically infected immunodeficient mice.

Then, we analyzed the intestinal antibody response and viral shedding in transferred immunodeficient mice. A low level of total human IgG was detected in fecal samples from mice dosed with PBMCs and with IgM$^+$ mBc, but not in those given Bc-dPBMCs or PBS (Fig. 4A). However, very little or no fecal human RV Ig was detected in any mice (Fig. 4A). Consistently, detection of RV Ag in stool showed that NOD/Shi-scid IL-2Rγ^{null} mice were chronically infected with RV at similar levels in all of the groups of mice evaluated (Fig. 4B).

Taken together, our data suggest that *in vivo*, during an RV infection, human IgM$^+$ mBc can differentiate into IgM and IgG ASCs and that the RV-specific antibodies secreted by these cells can significantly reduce antigenemia and viremia levels.

Human RV IgM$^+$ mBc are enriched in the IgM^{hi} IgD^{low} subset. Human IgM$^+$ mBc are heterogeneous, and at least three sub-

TABLE 2 Number of RV RNA-NSP5 copies/ml detected by quantitative RT-PCR in serum of mice passively transferred with PBS or indicated cell subsets

Transfer of:	Sample no.[a]	No. of copies/ml[b]
PBS	1	5.6×10^4
	2	8.6×10^4
	3	8×10^4
PBMCs	1	<25
	2	<25
	3	<25
Bc-dPBMc	1	2.3×10^4
IgM^+ mBc	1	<25
	2	<25

[a] Not enough sample was available from all mice, and only 9 of 16 samples were evaluated.
[b] Sensitivity limit of the assay, 25 copies/ml.

sets have been identified based on their expression of surface markers: $CD27^+$ IgM^+ IgD^- (IgM-only mBc), $CD27^+$ IgM^+ IgD^+ (a heterogeneous subset), and $CD27^+$ IgM^+ $CD43^{hi}$ (B1 cells) (15, 27, 34, 67). To determine if RV IgM^+ mBc were enriched in a particular IgM^+ mBc subset, we analyzed their phenotype by multiparametric FCA. In five experiments with cells from healthy adult volunteers, enrichment of RV-mBc was found in the IgM^+ IgD^+ subset, but not the IgM^+-only subset (Fig. 5A). When we analyzed the IgM^+ IgD^+ subset in more detail, RV-mBc were particularly enriched in the IgM^{hi} IgD^{low} subset (Fig. 5B). Of note, in these experiments the frequency of $CD27^+$ $CD43^{hi}$ B cells was very low (≤1% of purified B cells), the majority of them (>85%) did not express IgM, and RV-mBc were not enriched in this subset (data not shown). In conclusion, further characterization of circulating RV IgM^+ cells showed that such cells are enriched in the IgM^{hi} IgD^{low} subset, which has been previously shown to share

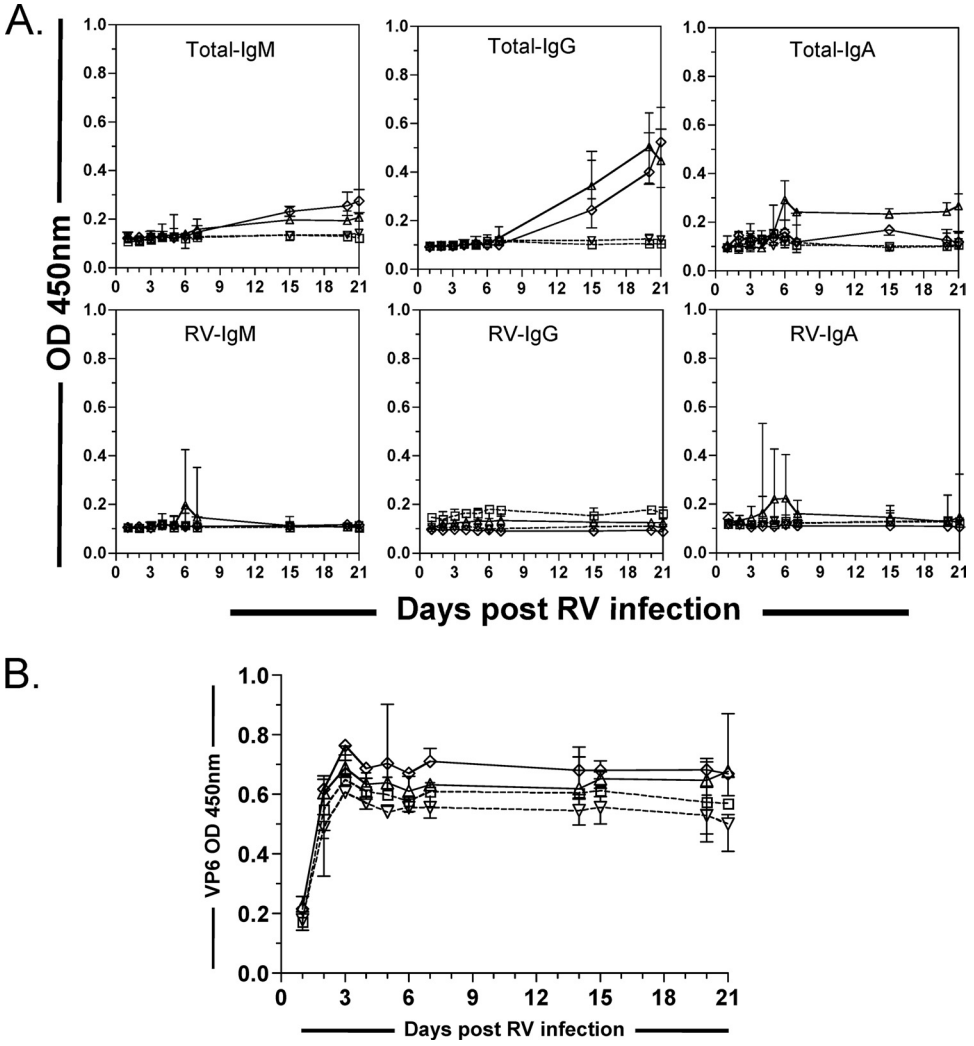

FIG 4 Transferred human B cells do not affect RV shedding in the stool. (A) Little or no human total (upper panel) or RV IgM, RV IgG, or RV IgA (lower panel) was detected in feces of immunodeficient mice after transfer. Relative quantities of total and RV IgM, RV IgG, and RV IgA were detected by ELISA in fecal samples collected 1 to 21 days postinfection in the four indicated groups of mice. (B) Relative quantities of RV VP6 detected by ELISA in fecal samples collected 1 to 21 days postinfection in the four indicated groups of mice. Immunodeficient NOD/Shi-scid IL-2Rγ^{null} mice were intraperitoneally inoculated with PBS (□, dashed line), PBMCs (△, continuous line), Bc-dPBMCs (▽, dashed line), or B-dPBMCs plus highly purified IgM^+ mBc (◇, continuous line) and immediately infected orally with the murine RV strain EC_{WT}. The median ($n = 4$) for each data point is presented.

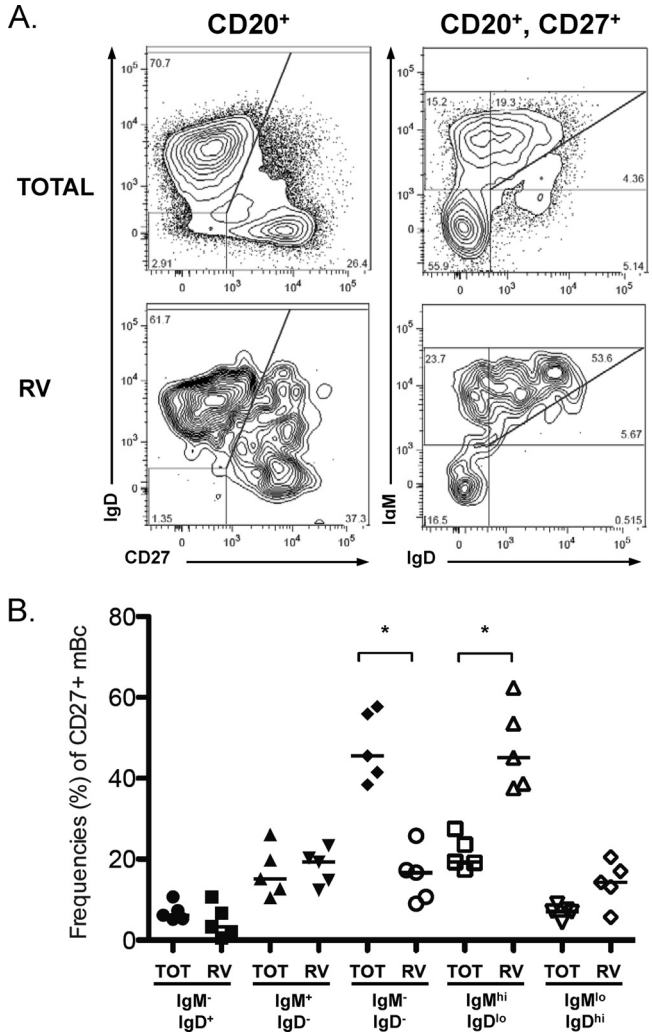

FIG 5 IgM$^+$ mBc are heterogeneous, and RV-specific mBc are enriched in the IgM^{hi} IgD^{low} subset. Rosette-enriched human B cells, like those used for the sorting experiments, were stained with GFP-VLPs, anti-CD20, anti-CD27, anti-IgD, and anti-IgM. (A) B cells (CD20$^+$) and mBc (CD20$^+$ CD27$^+$), total and RV-specific cells (GFP-VLP$^+$) were gated, and expression levels of IgD and IgM were analyzed for each subpopulation. One of five experiments performed is shown. (B) Summary of the frequencies (as percentages) of the five subsets of CD27$^+$ total and RV-mBc: IgM$^-$ IgD$^+$, IgM$^+$ IgD$^-$, IgM$^-$ IgD$^-$, IgM^{hi} IgD^{low}, and IgM^{low} IgD^{hi}. An asterisk indicates a significant difference ($P < 0.05$, Wilcoxon test). Median values are represented by the lines.

characteristics with marginal zone B cells (67), and that RV IgM$^+$ cells are not enriched in the recently described B1 cells (15, 27).

DISCUSSION

Previous studies by us and others have called attention to the high frequency and persistence of RV IgM$^+$ mBc in children and adults (53, 64). Despite their prominence, both the origin of these cells and their relevance to RV immunity have been unclear. IgM$^+$ mBc are peculiar in many ways: they rapidly differentiate to ASCs, they express CD27, and they have a high frequency of somatic hypermutations in the Ig heavy chain genes. These features support their classification as mBc (1, 34). However, the presence of these cells in the absence of a previous antigen exposure and the similar frequencies of somatic hypermutations in these cells from children and adults (68) do not support the view that they are true memory cells. The origin of these cells is also in dispute: the spleen has been shown to be important for the development and survival of these cells, and they may be circulating spleen marginal B cells (10, 67). IgM$^+$ mBc can be detected in patients that lack functional germinal centers due to genetic defects in genes of the CD40-CD40L pathway (67). Human IgM$^+$ mBc can be directly generated *in vitro* from transitional B cells stimulated with CpG, and for this reason they have been referred to as "natural memory B cells" (4). Human IgM$^+$ mBc express germinal center markers, and a genetic relationship has been described between clones of IgM$^+$ and switched mBc (55). Moreover, in mice it has been shown that IgM$^+$ mBc can restart a germinal center reaction and give rise to IgG$^+$ mBc (17). Nonetheless, a clonal relationship has not been found between IgM and switched mBc by other investigators (71). Thus, IgM$^+$ mBc are probably heterogeneous and may have multiple origins and serve multiple purposes, depending on the specific situation.

Isotype switching permits the generation of Igs with diverse effector functions (61). After stimulation of *in vitro*-purified IgM$^+$ mBc by using an optimized protocol, 62%, 21%, and 16% of total, RV, and tetanus toxoid mBc, respectively, that expressed IgM switched to express IgG; no switching to IgA expression was observed (Fig. 1B and C). IgA was not detected in the cultures of IgM$^+$ mBc, most likely because IgA switching requirements involve specific factors, such as APRIL and BAFF, produced from epithelial and local dendritic cells (28). The high purity of the starting mBc (Fig. 1A) and the high frequency of IgG$^+$, but not IgA$^+$, mBc observed after stimulation excludes the possibility that these cells were derived from contaminating switched cells in the initial cultures. Isotype switching of IgM$^+$ mBc to IgG-producing cells has also been observed in purified human B cells cocultured with an allorective T cell clone and in cultures in which IL-4 and CD40L were used for stimulation (37, 69). However, in another study, IgM$^+$ mBc stimulated with antibodies to BCR or CD40L did not switch to IgG expression and did not express AID, an enzyme required for the switching isotype (57). Similarly, single RV IgM$^+$ mBc, identified as CD19$^+$ IgD$^+$ CD27$^+$ GFP-VLP$^+$, expanded in response to IL-2, IL-4, and supernatant from mitogen-stimulated primary human T cells, and CD40L-transfected fibroblasts secreted IgM almost exclusively (64). Thus, the *in vitro* capacity of IgM$^+$ mBc to switch is probably highly dependent on the type of experimental stimuli used, and some previously reported results may have substantially underestimated this capacity. Although the possibility of isotype switching *in vitro* has been previously noted, this phenomenon has generally not been taken into account in the interpretation of assays in which mBc are quantified based on *in vitro* stimulation (2, 5, 9, 14). Our results suggest that an important fraction of mBc can switch *in vitro* under relatively optimized LDA stimulation conditions, and because of this ability the number of RV IgM$^+$ mBc has also been underestimated.

Although LDA studies of PBMCs have been extensively used to quantify total and antigen-specific mBc (5, 14, 53), the use of purified B cells is less common (2, 9), and a single study with purified mBc subsets has been previously described (52). While it was previously established that naive and mBc have different requirements for proliferation and effector activation (26), studies comparing cloning efficiencies of human mBc subsets by LDA are unusual (52). Here, we observed that total and RV IgM$^+$ mBc have

lower cloning efficiencies than switched mBc (Fig. 2). Differential expression of surface activator receptors and death susceptibility between the human mBc subsets could explain this finding. Purified IgG^+ mBc stimulated with R848 (an agonist of Toll-like receptor 7 [TLR7] and TLR8), high doses of IL-2, or autologous irradiated PMBCs as feeder cells (52) showed a similar cloning efficiency to the one we observed here (Fig. 2 and data not shown). It is clear, however, that only a fraction of mBc can be detected by functional LDA (52) and that the mBC capacity to switch confounds these studies. Obviously, this issue is further confounded, from a functional standpoint, by the fact that the crucial question of switch capacity *in vivo* may not be well reflected by any of the *in vitro* assays. Nevertheless, our studies have revealed a significant capacity of RV IgM^+ mBc to switch *in vitro* and this, coupled with the fact that these cells represent the most common RV-specific mBc in the circulation of children and adults, prompted us to determine whether these cells might also have a switch phenotype *in vivo*, as well as whether they were able to mediate any specific anti-RV functions.

An antimicrobial functional role for IgM^+ mBc has been previously demonstrated, especially against encapsulated bacteria (35, 58, 59). Nonetheless, the possible role of these cells in viral infections is not well understood. A heterosubtypic monoclonal antibody cloned from human IgM^+ mBc was protective against lethal challenge with influenza virus in mice (63). Also, it was recently proposed that IgM^+ mBc are involved in limiting the quantity of lipopolysaccharide that circulates in HIV-infected patients (40). The role of IgM^+ mBc in rotaviral immunity has been studied at several levels: clones of human RV IgM^+ mBc have been generated, and the antibodies they secrete were shown to be specific for RV VP6 (30, 64); most of the ASCs in acutely RV-infected children secrete IgM (25); finally, in mice a T cell-independent IgM response associated with protective immunity has been observed (8). Here, we extended these observations and showed that highly purified human IgM^+ mBc given intraperitoneally to immunodeficient mice that were subsequently infected with virulent murine RV switched to IgG *in vivo* (Fig. 3A). These findings are similar to previous observations with pneumococcal capsular antigen (46). The absence of tetanus toxoid IgM and little, if any, tetanus toxoid IgG in the IgM mBc recipient mice suggest that the stimulation and isotype switching were induced specifically by the ongoing RV infection.

Although several investigators have studied RV infection in immunodeficient mice (8, 22, 23) and NOD/Shi-scid IL-2Rγ^{null} mice have been used to study grafting of human cells (62), this is the first study reporting homologous murine RV infection in these mice. It is known that homologous EC_{WT} RV is highly virulent and is associated with high levels of viremia and viral shedding in the stool in wild-type and immunodeficient mice (6, 19). NOD/Shi-scid IL-2Rγ^{null} adult mice became chronically infected with EC_{WT}, and high levels of antigenemia and fecal RV antigens were detected on day 15 after infection in these mice (Fig. 3B and 4B). Although PBMCs depleted of B cells partially cleared the antigenemia, the presence of purified IgM^+ mBc significantly decreased the amount of serum RV VP6 and viral RNA compared to controls treated with PBS (Fig. 3B and Table 1), strongly suggesting a role for circulating IgM^+ mBc in the provision of systemic RV immunity. Consistent with our results, it was recently shown that in mice, murine lymphocytes are necessary to clear antigenemia but that neither T nor B cells are absolutely required for this effect (44).

Although neutralizing antibodies have been classically associated with control of viral replication in several RV models, inhibition of RV replication by nonneutralizing anti-VP6 antibodies has been previously demonstrated (21). Human circulating IgM^+ mBc are enriched in nonneutralizing anti-VP6 rather than neutralizing anti-VP4 or VP7-expressing cells (51, 64), and the anti-VP6 antibodies from these IgM^+ mBc are probably responsible for the decrease in circulating RV antigen. In support of this prediction, the transfer of both neutralizing and nonneutralizing antibodies to chronically infected immunodeficient mice delayed the onset and duration of antigenemia (44). Over 90% of acutely infected children have circulating RV antigen in their plasma, which disappears during the convalescence phase (7). The control of RV antigenemia is likely to be a critical component of RV immunity in both immunocompetent and immunodeficient children. Chronic systemic rotavirus infection associated with hepatitis and renal disease has been reported on multiple occasions in children with severe combined immunodeficiency (24). Extraintestinal manifestations of RV infection, like mild hepatitis, are very common (31), while convulsions (associated with viral antigen in spinal fluid) occur sporadically (16, 41). Modulation of the extent of systemic viral infection and its associated clinical sequelae is likely to be one of the effector functions of IgM^+ mBc.

Interestingly, fecal antigen shedding was not affected by transfer of IgM^+ mBc, probably because in these adult mice little if any human RV antibody reached the intestine (Fig. 4). To our knowledge, our study of the intestinal antibody response to viral infection in mice transferred human B cells has no precedent. Lack of effective transport of human Igs to the murine lumen and/or inefficient migration of transferred human B cells to the intestine (36) could explain our finding (Fig. 4).

We and others have reported that human circulating RV-specific cells are enriched in the $CD27^+$ IgM^+ subset (53, 64). Here, we extended these observations to show that this is primarily due to enrichment in the IgM^{hi} IgD^{low} mBc subset (Fig. 5). This phenotype is characteristic of marginal zone B cells, which also express high levels of CD21 (67). However, CD21 was not expressed at higher levels in this subset compared to other $CD27^+$ mBc subsets (data not shown). Human B1 cells have recently been reported to be $CD27^+$ IgM^+ $CD43^{high}$ (27). In our hands, the frequency of $CD27^+$ $CD43^{high}$ B cells was very low; the majority of them (>85%) did not express IgM, and they were not enriched in RV-mBc (data not shown). B1 cells defined with these markers are currently a subject of controversy, because they are easily contaminated with T cells and/or confused with plasma cells that have not completely lost CD20 (15). Thus, we conclude that RV-IgM^+ mBc are enriched in B cells with a phenotype similar to cells with an innate function (marginal zone B cells), but in this case, they have a substantial ability to switch *in vitro* and *in vivo* and to mediate antiviral immunity.

In summary, human circulating total and RV-IgM^+ mBc are enriched in the IgM^{hi} IgD^{low} subset, have differential cloning efficiencies, and can switch in *vitro* and *in vivo*. Moreover, the human IgM^+ mBc can mediate a significant reduction of RV antigenemia and viremia in immunodeficient mice, and therefore they are likely involved in immunity against RV.

ACKNOWLEDGMENTS

This study was supported by R01 AI-021362 and P30 DK56339-08 from the National Institutes of Health, by a VA Merit Review Award, and by FIRCA grant R03-TW05647-05. Carlos F. Narváez was funded by Colciencias and Stanford University Medical School.

We thank Lusijah Rott, Luz-Stella Rodríguez, Xiaosong He, Emily Deal, Olga L. Rojas, and Maria Jaimes for constructive suggestions.

REFERENCES

1. **Agematsu K, Hokibara S, Nagumo H, Komiyama A.** 2000. CD27: a memory B-cell marker. Immunol. Today **21**:204–206.
2. **Amanna IJ, Slifka MK.** 2006. Quantitation of rare memory B cell populations by two independent and complementary approaches. J. Immunol. Methods **317**:175–185.
3. **Angel J, Franco MA, Greenberg HB.** 2007. Rotavirus vaccines: recent developments and future considerations. Nat. Rev. Microbiol. **5**:529–539.
4. **Aranburu A, et al.** 2010. TLR ligation triggers somatic hypermutation in transitional B cells inducing the generation of IgM memory B cells. J. Immunol. **185**:7293–7301.
5. **Bernasconi NL, Traggiai E, Lanzavecchia A.** 2002. Maintenance of serological memory by polyclonal activation of human memory B cells. Science **298**:2199–2202.
6. **Blutt SE, Fenaux M, Warfield KL, Greenberg HB, Conner ME.** 2006. Active viremia in rotavirus-infected mice. J. Virol. **80**:6702–6705.
7. **Blutt SE, et al.** 2007. Rotavirus antigenemia in children is associated with viremia. PLoS Med. **4**:e121. doi:10.1371/journal.pmed.0040121.
8. **Blutt SE, Warfield KL, Lewis DE, Conner ME.** 2002. Early response to rotavirus infection involves massive B cell activation. J. Immunol. **168**: 5716–5721.
9. **Buisman AM, de Rond CG, Ozturk K, Ten Hulscher HI, van Binnendijk RS.** 2009. Long-term presence of memory B-cells specific for different vaccine components. Vaccine **28**:179–186.
10. **Carsetti R, Pantosti A, Quinti I.** 2006. Impairment of the antipolysaccharide response in splenectomized patients is due to the lack of immunoglobulin M memory B cells. J. Infect. Dis. **193**:1189–1190.
11. **Charpilienne A, et al.** 2001. Individual rotavirus-like particles containing 120 molecules of fluorescent protein are visible in living cells. J. Biol. Chem. **276**:29361–29367.
12. **Cherian T, Wang S, Mantel C.** 2012. Rotavirus vaccines in developing countries: the potential impact, implementation challenges, and remaining questions. Vaccine **30**(Suppl. 1):A3–A6.
13. **Coulson BS, Grimwood K, Hudson IL, Barnes GL, Bishop RF.** 1992. Role of coproantibody in clinical protection of children during reinfection with rotavirus. J. Clin. Microbiol. **30**:1678–1684.
14. **Crotty S, Aubert RD, Glidewell J, Ahmed R.** 2004. Tracking human antigen-specific memory B cells: a sensitive and generalized ELISPOT system. J. Immunol. Methods **286**:111–122.
15. **Descatoire, M, Weill JC, Reynaud CA, Weller S.** 2011. A human equivalent of mouse B-1 cells? J. Exp. Med. **208**:2563–2564. (Reply, 208:2566–2569.)
16. **DiFazio MP, Braun L, Freedman S, Hickey P.** 2007. Rotavirus-induced seizures in childhood. J. Child Neurol. **22**:1367–1370.
17. **Dogan I, et al.** 2009. Multiple layers of B cell memory with different effector functions. Nat. Immunol. **10**:1292–1299.
18. **Fecteau JF, Cote G, Neron S.** 2006. A new memory $CD27^-$ IgG^+ B cell population in peripheral blood expressing VH genes with low frequency of somatic mutation. J. Immunol. **177**:3728–3736.
19. **Fenaux M, Cuadras MA, Feng N, Jaimes M, Greenberg HB.** 2006. Extraintestinal spread and replication of a homologous EC rotavirus strain and a heterologous rhesus rotavirus in BALB/c mice. J. Virol. **80**:5219–5232.
20. **Feng N, et al.** 2008. Role of interferon in homologous and heterologous rotavirus infection in the intestines and extraintestinal organs of suckling mice. J. Virol. **82**:7578–7590.
21. **Feng N, et al.** 2002. Inhibition of rotavirus replication by a non-neutralizing, rotavirus VP6-specific IgA mAb. J. Clin. Invest. **109**:1203–1213.
22. **Franco MA, Greenberg HB.** 1997. Immunity to rotavirus in T cell deficient mice. Virology **338**:169–179.
23. **Franco MA, Greenberg HB.** 1995. Role of B cells and cytotoxic T lymphocytes in clearance of and immunity to rotavirus infection in mice. J. Virol. **69**:7800–7806.
24. **Gilger MA, et al.** 1992. Extraintestinal rotavirus infections in children with immunodeficiency. J. Pediatr. **120**:912–917.
25. **Gonzalez AM, et al.** 2003. Rotavirus-specific B cells induced by recent infection in adults and children predominantly express the intestinal homing receptor $\alpha4\beta7$. Virology **305**:93–105.
26. **Good KL, Avery DT, Tangye SG.** 2009. Resting human memory B cells are intrinsically programmed for enhanced survival and responsiveness to diverse stimuli compared to naive B cells. J. Immunol. **182**:890–901.
27. **Griffin DO, Holodick NE, Rothstein TL.** 2011. Human B1 cells in umbilical cord and adult peripheral blood express the novel phenotype $CD20^+$ $CD27^+$ $CD43^+$ CD70. J. Exp. Med. **208**:67–80.
28. **He B, et al.** 2007. Intestinal bacteria trigger T cell-independent immunoglobulin A(2) class switching by inducing epithelial-cell secretion of the cytokine APRIL. Immunity **26**:812–826.
29. **Jaimes MC, et al.** 2004. Maturation and trafficking markers on rotavirus-specific B cells during acute infection and convalescence in children. J. Virol. **78**:10967–10976.
30. **Kallewaard NL, et al.** 2008. Functional maturation of the human antibody response to rotavirus. J. Immunol. **180**:3980–3989.
31. **Kawashima H, et al.** 2012. Transaminase in rotavirus gastroenteritis. Pediatr. Int. **54**:86–88.
32. **Kim B, et al.** 2008. The influence of $CD4^+$ $CD25^+$ $Foxp3^+$ regulatory T cells on the immune response to rotavirus infection. Vaccine **26**:5601–5611.
33. **Klein U, Kuppers R, Rajewsky K.** 1997. Evidence for a large compartment of IgM-expressing memory B cells in humans. Blood **89**:1288–1298.
34. **Klein U, Rajewsky K, Kuppers R.** 1998. Human immunoglobulin $(Ig)M^+$ IgD^+ peripheral blood B cells expressing the CD27 cell surface antigen carry somatically mutated variable region genes: CD27 as a general marker for somatically mutated (memory) B cells. J. Exp. Med. **188**:1679–1689.
35. **Kruetzmann S, et al.** 2003. Human immunoglobulin M memory B cells controlling Streptococcus pneumoniae infections are generated in the spleen. J. Exp. Med. **197**:939–945.
36. **Kunkel EJ, Butcher EC.** 2003. Plasma-cell homing. Nat. Rev. Immunol. **3**:822–829.
37. **Lanzavecchia A.** 1983. One out of five peripheral blood B lymphocytes is activated to high-rate Ig production by human alloreactive T cell clones. Eur. J. Immunol. **13**:820–824.
38. **Lanzavecchia A, Parodi B, Celada F.** 1983. Activation of human B lymphocytes: frequency of antigen-specific B cells triggered by alloreactive or by antigen-specific T cell clones. Eur. J. Immunol. **13**:733–738.
39. **Leyendeckers H, et al.** 1999. Correlation analysis between frequencies of circulating antigen-specific IgG-bearing memory B cells and serum titers of antigen-specific IgG. Eur. J. Immunol. **29**:1406–1417.
40. **Lim A, et al.** 2011. Antibody and B-cell responses may control circulating lipopolysaccharide in patients with HIV infection. AIDS **25**:1379–1383.
41. **Liu B, et al.** 2009. Detection of rotavirus RNA and antigens in serum and cerebrospinal fluid samples from diarrheic children with seizures. Jpn. J. Infect. Dis. **62**:279–283.
42. **Madhi SA, et al.** 2010. Effect of human rotavirus vaccine on severe diarrhea in African infants. N. Engl. J. Med. **362**:289–298.
43. **Madhi SA, et al.** 2012. Efficacy and immunogenicity of two or three dose rotavirus-vaccine regimen in South African children over two consecutive rotavirus-seasons: a randomized, double-blind, placebo-controlled trial. Vaccine **30**(Suppl. 1):A44–A51.
44. **Marcelin G, Miller AD, Blutt SE, Conner ME.** 2011. Immune mediators of rotavirus antigenemia clearance in mice. J. Virol. **85**:7937–7941.
45. **McHeyzer-Williams LJ, McHeyzer-Williams MG.** 2004. Analysis of antigen-specific B-cell memory directly ex vivo. Methods Mol. Biol. **271**: 173–188.
46. **Moens L, Wuyts M, Meyts I, De Boeck K, Bossuyt X.** 2008. Human memory B lymphocyte subsets fulfill distinct roles in the anti-polysaccharide and anti-protein immune response. J. Immunol. **181**: 5306–5312.
47. **Narvaez CF, Angel J, Franco MA.** 2005. Interaction of rotavirus with human myeloid dendritic cells. J. Virol. **79**:14526–14535.
48. **Narvaez CF, Franco MA, Angel J, Morton JM, Greenberg HB.** 2010. Rotavirus differentially infects and polyclonally stimulates human B cells depending on their differentiation state and tissue of origin. J. Virol. **84**: 4543–4555.

49. **National Research Council.** 1996. Guide for the care and use of laboratory animals. National Academies Press, Washington, DC.
50. **Parashar UD, et al.** 2009. Global mortality associated with rotavirus disease among children in 2004. J. Infect. Dis. **200**(Suppl. 1):S9–S15.
51. **Parez N, et al.** 2004. The VP6 protein of rotavirus interacts with a large fraction of human naive B cells via surface immunoglobulins. J. Virol. **78**:12489–12496.
52. **Pinna D, Corti D, Jarrossay D, Sallusto F, Lanzavecchia A.** 2009. Clonal dissection of the human memory B-cell repertoire following infection and vaccination. Eur. J. Immunol. **39**:1260–1270.
53. **Rojas OL, Narvaez CF, Greenberg HB, Angel J, Franco MA.** 2008. Characterization of rotavirus specific B cells and their relation with serological memory. Virology **380**:234–242.
54. **Sasaki S, et al.** 2007. Comparison of the influenza virus-specific effector and memory B-cell responses to immunization of children and adults with live attenuated or inactivated influenza virus vaccines. J. Virol. **81**:215–228.
55. **Seifert M, Kuppers R.** 2009. Molecular footprints of a germinal center derivation of human IgM+(IgD+)CD27+ B cells and the dynamics of memory B cell generation. J. Exp. Med. **206**:2659–2669.
56. **Sen A, Pruijssers AJ, Dermody TS, Garcia-Sastre A, Greenberg HB.** 2011. The early interferon response to rotavirus is regulated by PKR and depends on MAVS/IPS-1, RIG-I, MDA-5, and IRF3. J. Virol. **85**:3717–3732.
57. **Shi Y, Agematsu K, Ochs HD, Sugane K.** 2003. Functional analysis of human memory B-cell subpopulations: IgD+CD27+ B cells are crucial in secondary immune response by producing high affinity IgM. Clin. Immunol. **108**:128–137.
58. **Shi Y, et al.** 2005. Regulation of aged humoral immune defense against pneumococcal bacteria by IgM memory B cell. J. Immunol. **175**:3262–3267.
59. **So NS, Ostrowski MA, Gray-Owen SD.** 2012. Vigorous response of human innate functioning IgM memory B cells upon infection by Neisseria gonorrhoeae. J. Immunol. **188**:4008–4022.
60. **Sow SO, et al.** 2012. Efficacy of the oral pentavalent rotavirus vaccine in Mali. Vaccine **30**(Suppl. 1):A71–A78.
61. **Stavnezer J, Guikema JE, Schrader CE.** 2008. Mechanism and regulation of class switch recombination. Annu. Rev. Immunol. **26**:261–292.
62. **Suemizu H, et al.** 2008. Establishment of a humanized model of liver using NOD/Shi-scid IL2Rγ^{null} mice. Biochem. Biophys. Res. Commun. **377**:248–252.
63. **Throsby M, et al.** 2008. Heterosubtypic neutralizing monoclonal antibodies cross-protective against H5N1 and H1N1 recovered from human IgM+ memory B cells. PLoS One **3**:e3942. doi:10.1371/journal.pone.0003942.
64. **Tian C, et al.** 2008. Immunodominance of the VH1-46 antibody gene segment in the primary repertoire of human rotavirus-specific B cells is reduced in the memory compartment through somatic mutation of non-dominant clones. J. Immunol. **180**:3279–3288.
65. **Velázquez FR, et al.** 1996. Rotavirus infections in infants as protection against subsequent infections. N. Engl. J. Med. **335**:1022–1028.
66. **Velazquez FR, et al.** 2000. Serum antibody as a marker of protection against natural rotavirus infection and disease. J. Infect. Dis. **182**:1602–1609.
67. **Weller S, et al.** 2004. Human blood IgM "memory" B cells are circulating splenic marginal zone B cells harboring a prediversified immunoglobulin repertoire. Blood **104**:3647–3654.
68. **Weller S, et al.** 2008. Somatic diversification in the absence of antigen-driven responses is the hallmark of the IgM+ IgD+ CD27+ B cell repertoire in infants. J. Exp. Med. **205**:1331–1342.
69. **Werner-Favre C, et al.** 2001. IgG subclass switch capacity is low in switched and in IgM-only, but high in IgD+IgM+, post-germinal center (CD27+) human B cells. Eur. J. Immunol. **31**:243–249.
70. **Wirths S, Lanzavecchia A.** 2005. ABCB1 transporter discriminates human resting naive B cells from cycling transitional and memory B cells. Eur. J. Immunol. **35**:3433–3441.
71. **Wu YC, et al.** 2010. High-throughput immunoglobulin repertoire analysis distinguishes between human IgM memory and switched memory B-cell populations. Blood **116**:1070–1078.
72. **Yen C, et al.** 2011. Rotavirus vaccines: update on global impact and future priorities. Hum. Vaccin. **7**:1282–1290.
73. **Youngman KR, et al.** 2002. Correlation of tissue distribution, developmental phenotype, and intestinal homing receptor expression of antigen-specific B cells during the murine anti-rotavirus immune response. J. Immunol. **168**:2173–2181.
74. **Zaman K, et al.** 2010. Efficacy of pentavalent rotavirus vaccine against severe rotavirus gastroenteritis in infants in developing countries in Asia: a randomised, double-blind, placebo-controlled trial. Lancet **376**:615–623.